through 20-gauge (nominal inner diameter: 0.6 mm) needles into rotating 40 wt.-% PEI (branched; average molecular weight, $M_w \sim 25\,000$; water-free; Aldrich) solutions in methanol.

The SWNT/PEI composite fibers were characterized by SEM (LEO 1590 VP microscope) and micro-Raman spectroscopy (Jobin–Yvon Horiba high-resolution LabRam micro-Raman spectrometer; helium–neon Spectra Physics laser, model 127, with excitation wavelength, $\lambda_{exc} = 632.8$ nm; resolution = ~ 1 cm^{-1}). The mechanical properties of these fibers were measured at room temperature with an Instron MicroTester (using a 1 cm gauge length and a constant strain rate of 0.9–1.2 % min^{-1}. Four-probe electrical conductivities were obtained from resistance values measured using a Keithley 2000 Multimeter and using the fiber-shell area (not including the area corresponding to the void space in the cross section). Thermal analysis was performed using a thermogravimetric analyzer (PerkinElmer Pyris 1 TGA) and a differential scanning calorimeter (PerkinElmer Pyris Diamond DSC).

Received: October 6, 2004
Final version: December 2, 2004

[1] R. H. Baughman, A. A. Zakhidov, W. A. de Heer, *Science* **2002**, *297*, 787.
[2] D. Qian, E. C. Dickey, R. Andrews, T. Rantell, *Appl. Phys. Lett.* **2000**, *76*, 2868.
[3] A. Allaoui, S. Bai, H. M. Cheng, J. B. Bai, *Compos. Sci. Technol.* **2002**, *62*, 1993.
[4] M. J. Biercuk, M. C. Llaguno, M. Radosavljevic, J. K. Hyun, A. T. Johnson, J. E. Fischer, *Appl. Phys. Lett.* **2002**, *80*, 2767.
[5] J. N. Coleman, W. J. Blau, A. B. Dalton, E. Muñoz, S. Collins, B. G. Kim, J. Razal, M. Selvidge, G. Vieiro, R. H. Baughman, *Appl. Phys. Lett.* **2003**, *82*, 1682.
[6] T. V. Sreekumar, T. Liu, B. G. Min, H. Guo, S. Kumar, R. H. Hauge, R. E. Smalley, *Adv. Mater.* **2004**, *16*, 58.
[7] B. Vigolo, A. Pénicaud, C. Coulon, C. Sauder, R. Pailler, C. Journet, P. Bernier, P. Poulin, *Science* **2000**, *290*, 1331.
[8] P. Poulin, B. Vigolo, P. Launois, *Carbon* **2002**, *40*, 1741.
[9] B. Vigolo, P. Poulin, M. Lucas, P. Launois, P. Bernier, *Appl. Phys. Lett.* **2002**, *81*, 1210.
[10] A. B. Dalton, S. Collins, E. Muñoz, J. M. Razal, V. H. Ebron, J. P. Ferraris, J. N. Coleman, B. G. Kim, R. H. Baughman, *Nature* **2003**, *423*, 703.
[11] A. B. Dalton, S. Collins, J. Razal, E. Muñoz, V. H. Ebron, B. G. Kim, J. N. Coleman, J. P. Ferraris, R. H. Baughman, *J. Mater. Chem.* **2004**, *14*, 1.
[12] E. Muñoz, A. B. Dalton, S. Collins, M. Kozlov, J. Razal, J. N. Coleman, B. G. Kim, V. H. Ebron, M. Selvidge, J. P. Ferraris, R. H. Baughman, *Adv. Eng. Mater.* **2004**, *6*, 801.
[13] V. A. Davis, L. M. Ericson, A. N. G. Parra-Vasquez, H. Fan, Y. Wang, V. Prieto, J. A. Longoria, S. Ramesh, R. K. Saini, C. Kittrell, W. E. Billups, W. W. Adams, R. H. Hauge, R. E. Smalley, M. Pasquali, *Macromolecules* **2004**, *37*, 154.
[14] L. M. Ericson, H. Fan, H. Peng, V. A. Davis, W. Zhou, J. Sulpizio, Y. Wang, R. Booker, J. Vavro, C. Guthy, A. N. G. Parra-Vasquez, M. J. Kim, S. Ramesh, R. K. Saini, C. Kittrell, G. Lavin, H. Schmidt, W. W. Adams, W. E. Billups, M. Pasquali, W.-F. Hwang, R. H. Hauge, J. E. Fischer, R. E. Smalley, *Science* **2004**, *305*, 1447.
[15] J. Kong, N. R. Franklin, C. Zhou, M. G. Chapline, S. Peng, K. Cho, H. Dai, *Science* **2000**, *287*, 622.
[16] M. Shim, A. Javey, N. W. S. Kam, H. Dai, *J. Am. Chem. Soc.* **2001**, *123*, 11 512.
[17] E. V. Basiuk, V. A. Basiuk, J.-G. Bañuelos, J.-M. Saniger-Blesa, V. A. Pokrovskiy, T. Y. Gromovoy, A. V. Mischanchuk, B. G. Mischanchuk, *J. Phys. Chem. B* **2002**, *106*, 1588.
[18] J. Sun, L. Gao, *Carbon* **2003**, *41*, 1063.
[19] A. Star, J.-C. P. Gabriel, K. Bradley, G. Grüner, *Nano Lett.* **2003**, *3*, 459.
[20] D. Chattopadhyay, I. Galeska, F. Papadimitrakopoulos, *J. Am. Chem. Soc.* **2003**, *125*, 3370.
[21] A. A. Mamedov, N. A. Kotov, M. Prato, D. M. Guldi, J. P. Wicksted, A. Hirsch, *Nat. Mater.* **2002**, *1*, 190.
[22] A. V. Neimark, S. Ruetsch, K. G. Kornev, P. I. Ravikovitch, P. Poulin, S. Badaire, M. Maugey, *Nano Lett.* **2003**, *3*, 419.
[23] P. Nikolaev, M. J. Bronikowski, R. Kelley Bradley, F. Rohmund, D. T. Colbert, K. A. Smith, R. E. Smalley, *Chem. Phys. Lett.* **1999**, *313*, 91.
[24] A. Thess, P. Nikolaev, H. J. Dai, P. Petit, J. Robert, C. H. Xu, Y. H. Lee, S. G. Kim, A. G. Rinzler, D. T. Colbert, G. E. Scuseria, D. Tománek, J. E. Fischer, R. E. Smalley, *Science* **1996**, *273*, 483.
[25] G. R. Dieckmann, A. B. Dalton, P. A. Johnson, J. Razal, J. Chen, G. M. Giordano, E. Muñoz, I. H. Musselman, R. H. Baughman, R. K. Draper, *J. Am. Chem. Soc.* **2003**, *125*, 1770.
[26] M. Cadek, J. N. Coleman, V. Barron, K. Hedicke, W. J. Blau, *Appl. Phys. Lett.* **2002**, *81*, 5123.
[27] A. Sotelo, G. F. de la Fuente, F. Lera, D. Beltrán, F. Sapiña, R. Ibáñez, A. Beltrán, M. R. Bermejo, *Chem. Mater.* **1993**, *5*, 851.
[28] R. Tanaka, H. Yamamoto, A. Shono, K. Kubo, M. Sakurai, *Electrochim. Acta* **2000**, *45*, 1385.
[29] D. Schoolmann, O. Trinquet, J.-C. Lassègues, *Electrochim. Acta* **1992**, *37*, 1619.
[30] C. S. Harris, M. A. Ratner, D. F. Shriver, *Macromolecules* **1987**, *20*, 1778.
[31] J.-L. Paul, C. Jegat, J.-C. Lassègues, *Electrochim. Acta* **1992**, *37*, 1623.
[32] A. G. Rinzler, J. Liu, H. Dai, P. Nikolaev, C. B. Huffman, F. J. Rodríguez-Macías, P. J. Boul, A. H. Lu, D. Heymann, D. T. Colbert, R. S. Lee, J. E. Fischer, A. M. Rao, P. C. Eklund, R. E. Smalley, *Appl. Phys. A* **1998**, *67*, 29.

An Axisymmetric Flow-Focusing Microfluidic Device**

By *Shoji Takeuchi*, *Piotr Garstecki*, *Douglas B. Weibel*, and *George M. Whitesides**

This paper describes a microfluidic axisymmetric flow-focusing device (AFFD) fabricated in poly(dimethylsiloxane) (PDMS) that produces polymer-coated droplets with size distributions significantly more narrow than those generated using conventional microencapsulation methods.[1–3] The AFFD confines droplets in the central axis of a microfluidic channel; this confinement protects droplets from shear, or from damage re-

[*] Prof. G. M. Whitesides, Dr. S. Takeuchi, Dr. P. Garstecki, Dr. D. B. Weibel
Department of Chemistry and Chemical Biology
Harvard University, 12 Oxford St., Cambridge, MA 02138 (USA)
E-mail: gwhitesides@gmwgroup.harvard.edu
Dr. S. Takeuchi
Institute of Industrial Science, The University of Tokyo
4-6-1 Komaba, Meguro-ku, Tokyo 153-8505 (Japan)

[**] This research was supported by DARPA. S.T. received an overseas research scholarship from the Ministry of Education, Culture, Sports, Science and Technology of Japan. P.G. thanks the Foundation for Polish Science for a postdoctoral fellowship. D.B.W was a recipient of a postdoctoral fellowship from the National Institutes of Health (GM067445).

 DOI: 10.1002/adma.200401738 © 2005 WILEY-VCH Verlag GmbH & Co. KGaA, Weinheim

ADVANCED MATERIALS

sulting from adhesion or wetting at the walls of the outlet channel. Avoiding contact of the droplets with the walls is important for two other reasons: i) it prevents the dispersed phase from wetting the walls of the channels;[4] and ii) it protects the nascent surface of the polymer film early in the interfacial polymerization reaction, when the film is fragile and contact with the wall may disrupt the membrane. These characteristics allow the AFFD to produce microencapsulated droplets of liquids that are difficult to obtain in quasi-two-dimensional microfluidic devices fabricated in PDMS. We have used the AFFD to make aqueous droplets containing ions or superparamagnetic particles encapsulated in nylon-6,6 membranes by carrying out interfacial polymerization reactions in situ.

Microencapsulation has many important industrial applications.[5] In biomedical engineering, microcapsules with semipermeable membranes, including polyamides,[1–3,6,7] polyelectrolytes,[8] and colloidal membranes,[9] have been useful materials for the timed release of substances,[3,10] and for modeling artificial cells.[6,7] One important criterion in producing encapsulated droplets for these biomedical applications is size uniformity. Uniform diffusion profiles and targeting efficiency[11] are characteristics that are strongly dependent on the size of particles used in drug delivery. The control over the rheological properties or stability of emulsions is also influenced by the distribution of droplet size.[12] Microcapsules with uniform dimensions are, thus, important materials in food science, printing, adhesives, cosmetics, toothpaste, explosives, pesticides, and in other areas.[5]

Conventional methods of encapsulating micrometer-sized droplets—including agitation,[2] spray drying,[13] and membrane emulsification[1,3,14,15]—produce polymer-coated microcapsules with a coefficient of variation (CV) of the diameter between 10 and 50%;[1,6,13,15] CV is defined by $CV = (\sigma_d / \langle d \rangle) \times 100$, where σ_d is the standard deviation of the diameter, and $\langle d \rangle$ is its mean value. Other flow-focusing techniques that produce monodisperse droplets exist.[16] These methods do not allow polymerization reactions at the surface of particles to be carried out in situ, and are not easily configured for microfluidic systems. This paper describes a microfluidic AFFD that produces Nylon-coated microcapsules with a CV of approximately 5 %.

Microfluidic flow-focusing devices can produce monodisperse droplets ($CV < 5\,\%$) at a high frequency ($\approx 10^3\ s^{-1}$), and with the characteristic that the size of particles can be controlled by controlling the flow rates.[17] Microfluidic devices for making droplets that have been described to date are based on quasi-two-dimensional (2D), planar channels, and are usually fabricated in PDMS (Fig. 1a,b).[17] Two-dimensional microfluidic devices offer the advantages of ease of fabrication and visualization.[17] For the preparation of polymer-coated microcapsules, however, they have two significant drawbacks: i) contact of the discontinuous phase with the walls of the channel limits the fluids that can be used to generate droplets, and ii) leaking can occur at the interface between the layers of PDMS used to fabricate the device at high flow rates and pressures.[18]

When the discontinuous phase wets the walls of the channels, its capillary instability is altered, and the process of break-up is difficult to control.[1,19] In contrast, when the discontinuous phase is surrounded entirely by the continuous phase, the process of break-up is stable.[16] The problems with the wetting of surfaces can, in principle, be eliminated by the judicious choice of surfactants; in practice, however, eliminating problems with wetting can be difficult when one or more of the *reagents* also exhibits surface-active properties. As the science of wetting and surface affinity still has empirical elements, finding the proper combination of reactants and surfactants can be frustrating. As an example, we found that aqueous solutions of 1,6-diaminohexane (0.1 M, pH ~ 12.35)—a monomer used in the synthesis of nylon-6,6—exhibited a high affinity for oxidized PDMS,[20] and consequently wet the walls of 2D channels composed of PDMS, even in the presence of surfactant. Silanizing the walls solved this problem only temporarily. Planar microfluidic devices fabricated in PDMS were incompatible with this class of reactants.

When droplets coated with nylon made contact with the walls of microfluidic channels, shear stress destroyed the polymer coating (Fig. 1a, cross-sectional view). To avoid contact

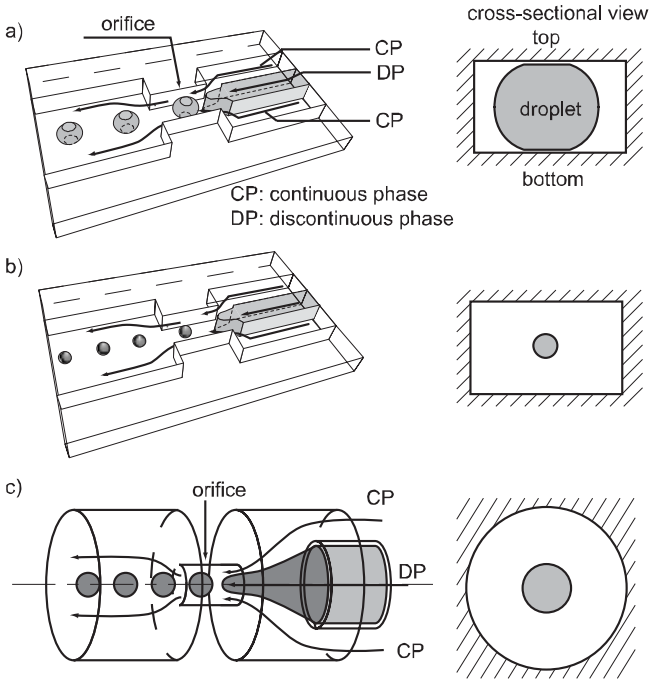

Figure 1. Schematic illustrations of 2D and three-dimensional (3D) microfluidic channels, and a cross-sectional view of a 3D device with a droplet. a) A conventional flow-focusing channel (2D). The discontinuous phase is broken into droplets by the continuous phase. A droplet usually contacts at least two (top and bottom) walls of the channels. In this case, shear stress between the wall and the droplet ruptures the polymerizing shell of nylon. b) Small droplets produced at high flow rates of the continuous phase do not experience shear stress with the walls; at these flow rates, leaking is a problem in 2D channels. c) An axisymmetrical flow focusing channel (3D). The channel is composed of a cylindrical tube with a narrow cross-section halfway down its length. The narrow region serves as the orifice where fluid is focused and breaks into aqueous droplets. In this geometry, wetting problems are avoided since the aqueous phase does not make contact with the walls.

 © 2005 WILEY-VCH Verlag GmbH & Co. KGaA, Weinheim

between the droplets and the walls, we produced droplets much smaller than the height of the device by varying the flow rates (Fig. 1b). Unfortunately, however, the pressure drop along the channels that accompanied higher flow rates often caused fluid to leak from the PDMS/PDMS or PDMS/glass seals.

Here, we approach these problems geometrically. In the AFFD shown in Figure 1c, the inner aqueous phase is surrounded by the continuous phase and never touches the walls; thus wetting does not occur. Droplets coated with nylon do not contact the walls of the channel in the AFFD, and thus avoid the regions of highest shear. This device is also fabricated from a single piece of PDMS, rather than by bonding two layers together. Since the channel is seamless, it does not leak at high flow rates and pressures; this feature allowed us to produce droplets of liquid encapsulated in nylon-6,6 with a diameter greater than 50 μm.

Figure 2a sketches the fabrication of the AFFD and Figure 2b illustrates a complete device with two inserted glass capillaries serving as an inlet and outlet. We used an optical fiber 0.25 mm in diameter covered with a 0.75 mm thick layer of insulation as a master for the channel. A section of the insulation was cut back using a scalpel and removed to expose a region of the optical fiber. The fiber was molded in PDMS, and after curing, the insulation and fiber were removed from the PDMS slab by pulling the fiber and insulation out from one side of the orifice, leaving the insulation on the other side intact; the insulation on the other side was subsequently removed. The narrow, central part of the channel served as the orifice; the size of the orifice can be reduced by using an optical fiber or insulated wire with a smaller diameter. The channel has three inlets and one outlet (see Fig. 2 for further details). We formed an inlet for the discontinuous phase and an outlet for the droplets by inserting glass capillaries (0.75 mm outer diameter, 0.5 mm inner diameter) into both sides of the orifice. The two inlets for the continuous phase were formed by drilling holes into the channel and connecting polyethylene tubing to the holes. In this configuration, we were able to introduce three separate solutions into the channel.

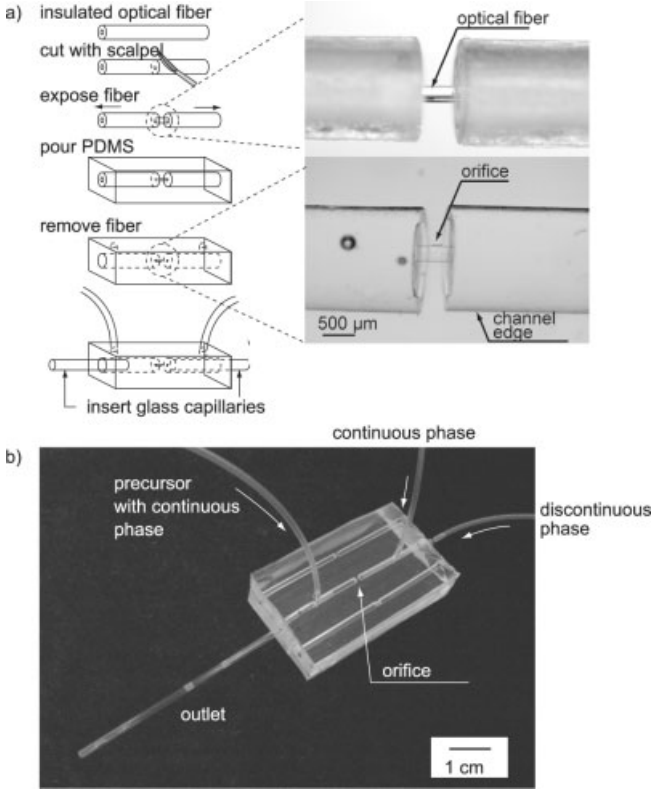

Figure 2. a) A scheme depicting the fabrication process of the AFFD. The insulation surrounding an optical fiber (0.25 mm in diameter covered with a 0.75 mm thick layer) was cut with a scalpel and the ends pulled to expose the fiber. The fiber was embedded in a block of PDMS ($3 \times 6 \times 1.5$ cm^3). After the PDMS had cured, the fiber was removed by pulling the fiber out through the end of the PDMS block. Two glass capillaries (0.75 mm outer diameter, 0.5 mm inner diameter) were inserted as an inlet and outlet. b) An image of the final AFFD.

Figure 1c illustrates the details of the design of the AFFD. To prepare droplets in the AFFD, we delivered an aqueous solution of 1,6-diaminohexane (0.1 M) to the orifice from a capillary placed axisymmetrically in the flow tube. We used a solution of Span-80 (2 % v/v) in hexadecane as the continuous phase. As the continuous phase flowed around the capillary, the aqueous phase formed a cylindrical thread that periodically entered the orifice, broke, and released droplets into the downstream portion of the flow tube (outlet channel). The break-up process was stable, and the aqueous phase did not wet the walls of the channel, even at low flow rates.

Figures 3a–c illustrate the variation in the size of the droplets formed in an AFFD positioned horizontally and vertically. Using a 250 μm diameter orifice, we formed droplets 50–300 μm in diameter by varying the flow rate of the continuous phase between 1–50 mL h^{-1}. The diameter of the droplets decreased as the flow rate of the continuous phase was increased.

When the device was oriented horizontally, we observed that the droplets accumulated on the wall of the outlet channel (Fig. 3b); accumulation caused the droplets to collapse during the early stage of the polymerization. In order to avoid this problem, we reoriented the device vertically and observed that the droplets followed the centerline of the channel and flowed one-by-one to the outlet (Fig. 3c).

Surprisingly, we found that the size of droplets formed in a vertically oriented AFFD were smaller than those formed at the same flow rates (of both phases) in an AFFD oriented horizontally. In order to assess the origin of this difference, we evaluated whether gravity had any influence on the break-up process; it did not. This was demonstrated by calculating the Bond (Bo) number, a dimensionless quantity that describes the relative importance of gravitational and interfacial forces. We determined Bo using the equation, $\mathrm{Bo} = g \cdot \Delta\varrho \cdot L^2/\gamma$, where g is the gravitational acceleration ($g \approx 9.8$ m s^{-2}), $\Delta\varrho$ is the difference of densities of the aqueous and organic phase ($\varrho_{\mathrm{water}} \sim 1$ g cm^{-3}, $\varrho_{\mathrm{hexadecane}} \sim 0.77$ g cm^{-3}, $\Delta\varrho \approx 3 \times 10^2$ kg m^{-3}), and γ is the surface tension ($\gamma \approx 3 \times 10^{-2}$ N m^{-1}). For a typical length scale, L, of the interface during break-up, we used the width of the orifice

 © 2005 WILEY-VCH Verlag GmbH & Co. KGaA, Weinheim

ADVANCED MATERIALS

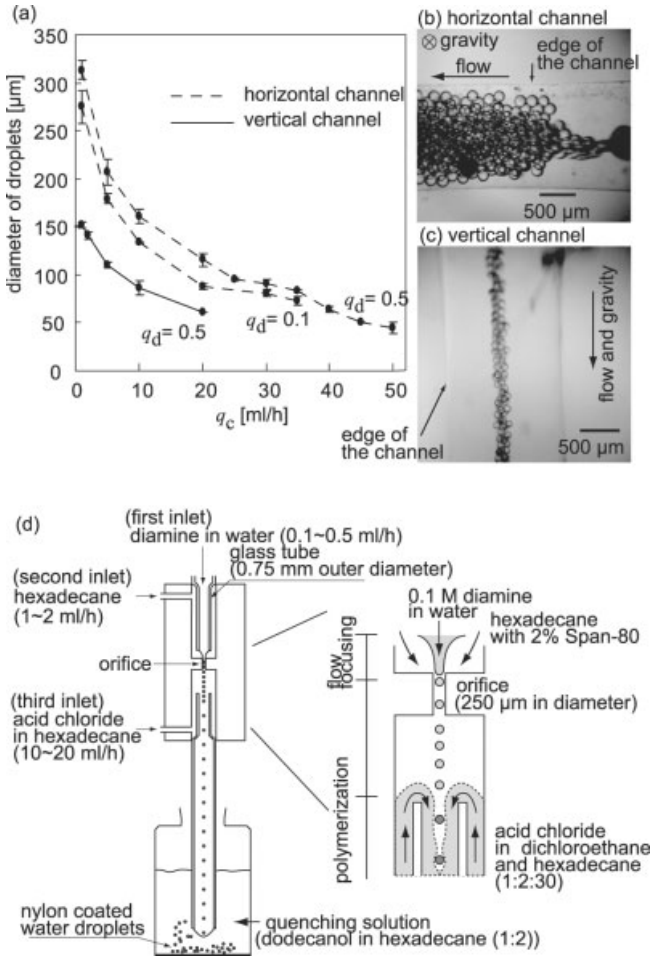

Figure 3. a) The diameter of the droplets at the various flow rates of the continuous phase (q_c). The diameter of the orifice was 250 μm; q_d represents the flow rate of the discontinuous phase. The continuous phase was a solution of Span-80 in hexadecane (2 % v/v). The discontinuous phase was an aqueous solution of 1,6-hexanediamine (0.1 M). b,c) Images showing droplets created in the AFFD oriented (b) horizontally and (c) vertically at flow rates of 10 mL h^{-1} for both the continuous and discontinuous phases. In the channel oriented horizontally, the direction of gravity is orthogonal to the plane of the page; in the channel oriented vertically, the direction is in the plane of the page and indicated by the arrow. d) A schematic diagram of the AFFD used to prepare nylon-6,6-coated aqueous droplets. An aqueous solution of 1,6-diaminohexane (0.1 M) was introduced into the channel at the first inlet. The continuous phase, Span-80 in hexadecane (2 % v/v), was introduced into the channel from a second set of inlets. A solution of adipoyl chloride in dichloroethane and hexadecane (1:2:30) was introduced into the channel from a third inlet. Polymerization of adipoyl chloride and 1,6-diaminohexane occurred on the surface of the droplets. A solution of dodecanol in hexadecane (30 % v/v) was used to quench the polymerization reaction.

w_{or} ($L = w_{or} \approx 10^{-4}$ m). (The actual radii of curvature of the collapsing neck of the inner stream are smaller than the width of the orifice. Taking $L = w_{or}$ overestimates the influence of gravity (body force) over interfacial tension (surface force).) In our device, a typical value of the Bond number was 10^{-3}; this implies that gravity, and thus the orientation of the device, does not influence the process of break-up directly.

We find, however, that the orientation has a large impact on the flow of the droplets in the outlet channel. These droplets are heavier than the continuous phase, and in a device oriented horizontally, the droplets settled against the floor on the channel where they formed a high volume fraction emulsion; the emulsion eventually filled the entire cross-section of the channel (Fig. 3b). This emulsion altered the flow of the continuous fluid, and provided a higher resistance to flow in the outlet channel; this increased the pressure in the orifice region. We believe that it is only in this *indirect* way that gravity influences the break-up process and leads to the difference in the size of droplets produced in devices oriented horizontally and vertically.

We have used the vertical AFFD to prepare droplets coated with nylon-6,6 via the interfacial polymerization of adipoyl chloride in the continuous, hexadecane phase and 1,6-diaminohexane in the discontinuous, aqueous phase (Fig. 3d). In order to avoid problems associated with rapid polymerization in the orifice, we formed aqueous droplets of 1,6-diaminohexane in hexadecane, and included an additional capillary at the outlet region of the flow channel to introduce a stream of adipoyl chloride in dichloroethane/hexadecane.

In this configuration, aqueous droplets suspended in the continuous phase (2 % Span-80 in hexadecane) flowed into the outlet capillary together with a solution of adipoyl chloride in dichloroethane and hexadecane (1:2:30 v/v). When adipoyl chloride contacted the surface of the aqueous droplets, the interfacial polymerization proceeded rapidly, and produced droplets uniformly coated with nylon-6,6 within the channel. The outlet of the capillary was immersed in a beaker containing a solution of dodecan-1-ol in hexadecane (30 % v/v) that quenched unreacted adipoyl chloride, and terminated the polymerization reaction. In the absence of a quenching agent, the polymerization proceeded until all of the diamine had diffused out of the droplet. By quenching the polymerization, we avoided droplets becoming crosslinked as they came into contact in the collection beaker. This quenching reaction might be used to modify the properties of the membrane by including appropriate reactants in the quenching reaction.

Using the experimental device described in Figure 3d, we produced nylon-6,6-coated aqueous droplets (50–300 μm diameter) at a rate of ~500 droplets per minute; the process operated without blocking or interruption for >6 h (generating $>10^5$ droplets). Figure 4a shows photomicrographs of the microencapsulated droplets. Approximately 10 % of the nylon-coated droplets collapsed or deformed during the polymerization. We suspect that this damage may be due to aggregation of the droplets during the polymerization step. Most of the remaining microcapsules (90 %) were perfectly spherical with a uniform diameter.

Figures 4c,d illustrate the size distribution of the droplets as they were generated at the orifice, and after the nylon membrane had formed. To determine the distribution, we measured the diameter of individual droplets produced at the orifice and encapsulated droplets that were neither deformed nor broken. In this experiment, we omitted droplets that were

 © 2005 WILEY-VCH Verlag GmbH & Co. KGaA, Weinheim

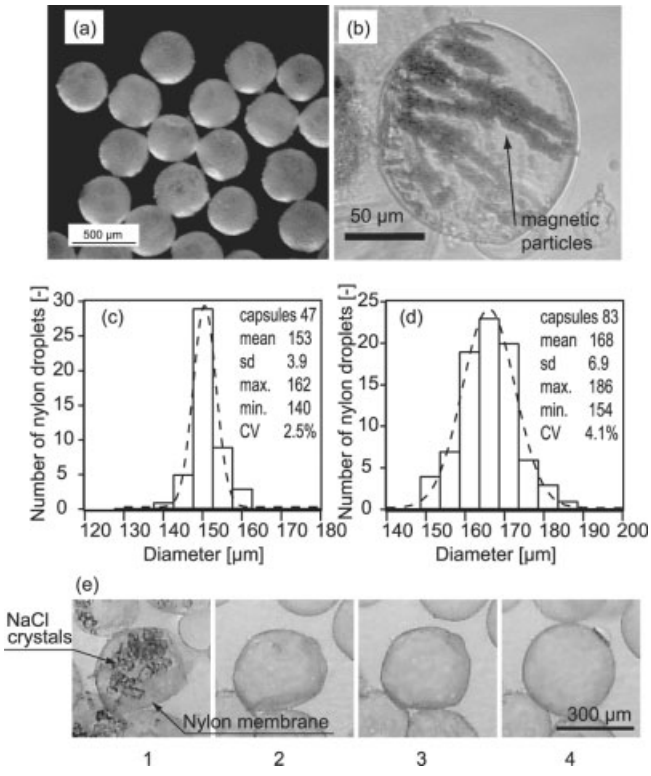

Figure 4. a) A collection of nylon-6,6-coated aqueous droplets. b) A coated-droplet containing 50 nm diameter magnetic particles in an applied magnetic field. The particles are aligned with respect to the magnetic field. c,d) Distributions of the diameter of droplets before (c) and after (d) polymerization. The droplets were prepared in a vertically oriented flow-focusing device using hexadecane as the continuous phase (flow rate, 5 mL h^{-1}), and 1,6-diaminohexane as the discontinuous phase (flow rate, 0.5 mL h^{-1}). The diameters of each droplet were measured using video analysis software (Scion Image). The error in measurements was approximately 5 µm. (sd: standard deviation, CV: coefficient of variation.) e) A swelling experiment of nylon-encapsulated solutions of NaCl. Encapsulated solutions of sodium chloride were dehydrated by adding ethanol. The resulting nylon membranes were filled with crystals of sodium chloride (frame 1). The solvent was exchanged for water, and the membrane was imaged over time as it swelled. The total time lapsed between frames 1 and 4 is approximately 30 s. In frame 4, the membrane is fully swelled and spherical. The scale bar in frame 4 is 300 µm.

deformed or collapsed (< 10 % of the droplets produced). Although the deviation in the diameter of the droplets becomes larger after polymerization (CV = 4.1 %) compared with that before (2.5 %), it is small and on the order of the error of the measurement. A coefficient of variance of < 5 % is the commonly accepted definition of monodispersity.[21]

Using the AFFD, we were able to control the size of the droplets and carry out polymerizations on the surface of droplets. To demonstrate the versatility of this process, we encapsulated micro- and nanoparticles inside nylon membranes by mixing the particles into the discontinuous phase. Figure 4b illustrates a nylon-encapsulated droplet containing a ferrofluid—superparamagnetic iron oxide particles ~ 50 nm in diameter stabilized with a surfactant—in an external magnetic field. When we applied an external magnetic field, the magnetic particles inside the droplets aligned, and moved toward the magnetic field. In contrast to the membrane during polymerization, the polymer membrane after polymerization was strong and did not break when we manipulated the capsules with a magnetic field.

An interesting property of nylon membranes is their semipermeability. We added sodium chloride to the discontinuous phase (2 %) and prepared salt solutions encapsulated in nylon-coated droplets. When we dehydrated the droplets in ethanol, the nylon membranes collapsed and the collapsed capsules filled with crystals of sodium chloride. When the membranes were re-suspended in water, the osmotic pressure across the nylon membrane caused them to expand and fill with water, until they again formed spherical particles; remarkably, the nylon membranes did not break during collapse and subsequent swelling. Figure 4e illustrates a sequence of images depicting the hydration of a nylon-6,6 membrane containing sodium chloride crystals. The hydration of salt crystals within the permeable membrane produced polymer-coated droplets with few defects. This phenomenon may be a useful model for studying 'osmophoresis'—the osmotic motion of cells or small capsules in concentration gradients.[22]

In conclusion, we have fabricated axisymmetrical microfluidic flow-focusing devices in PDMS and have used them to prepare nylon-6,6-coated aqueous droplets with narrow size distributions. This approach has two primary advantages over conventional 2D microfluidic systems: i) the use of an axisymmetric channel avoids both the problems associated with wetting the channel walls and the collapse of polymerizing droplets due to shear at the walls; ii) channels embedded in a solid slab of PDMS allow us to operate at both high and low pressure without problems associated with fluid leaking at seals. We believe that the geometry of the AFFD can be used to prepare encapsulated, monodisperse droplets by polymerization or precipitation reactions from a variety of reactants.[23] The fabrication of AFFD devices in PDMS is simple—molding optical fibers or insulated wires—and does not require expensive equipment. Using dimensions other than those available in optical fibers and insulated wires would require fabricating appropriate systems. It is also difficult (depending on the design) to fabricate AFFDs with complicated patterns of channels or with several junctions, each delivering different reagents. The application of other microfabrication techniques—stereolithography, deep reactive ion etching, three-dimensional electroplating, among others—may provide a route to fabricating masters for these more complicated AFFDs. (While this paper was being revised to take into account referee's comments, Beebe and colleagues published a description of the use of a similar microfluidic system to make continuous tubes.[24])

Experimental

We fabricated channels by embedding insulated optical fibers in PDMS (Sylgard 184, Dow Corning). Insulated optical fibers were prepared by inserting an optical fiber (Fiber optics SMF-28-09, Thorlabs

 © 2005 WILEY-VCH Verlag GmbH & Co. KGaA, Weinheim

ADVANCED MATERIALS

Inc) into polyethylene tubing (PE90, Becton Dickinson and Company) that was filled with pre-epoxy (5 minute Epoxy, Devcon). The use of polyethylene tubing as the insulating layer resulted in channels that were wide enough for us to insert glass capillaries directly, to serve as inlet/outlet channels. Holes for the inlets for the continuous phase were drilled with a needle ($60^{1/2}$, Becton Dickinson and Company), and polyethylene tubing (PE60) was inserted into the holes. Syringe pumps (PHD2000, Harvard Apparatus) were used to control the flow of fluids.

Images of nylon-coated droplets were collected with a charge-coupled device (CCD) camera (DMX1200, Nikon) connected to a stereo- or inverted microscope. The diameter of the droplets was measured by analyzing the images (Scion Image, Scion Corporation).

Received: October 21, 2004
Final version: December 16, 2004

[1] N. Yamazaki, K. Nagashima, M. Nagai, G.-H. Ma, S. Omi, *J. Dispersion Sci. Technol.* **2003**, *24*, 249.
[2] S. Alexandridou, C. Kiparissides, F. Mange, A. Foissy A, *J. Microencapsul.* **2001**, *18*, 767.
[3] L.-Y. Chu, S.-H. Park, T. Yamaguchi, S. Nakao, *Langmuir* **2002**, *18*, 1856.
[4] R. Dreyfus, P. Tabeling, H. Willaime, *Phys. Rev. Lett.* **2003**, *90*, 144 505.
[5] a) R. Arshady, *J. Microencapsul.* **1993**, *10*, 413. b) F. Giroud, J. M. Pernot, H. Brun, B. Pouyet, *J. Microencapsul.* **1995**, *12*, 389. c) P. B. O'Donnell, J. W. Mcginity, *Adv. Drug Delivery Rev.* **1997**, *28*, 25. d) E. L. Chaikof, *Annu. Rev. Biomed. Eng.* **1999**, *1*, 103. e) L. S. Jackson, K. Lee, *Food Sci. Technol.* **1991**, *24*, 289.
[6] D. Poncelet, R. J. Neufeld, *Biotechnol. Bioeng.* **1987**, *33*, 95.
[7] T. M. S. Chang, *Science* **1964**, *146*, 524.
[8] a) C. S. Peyratout, L. Dahne, *Angew. Chem. Int. Ed.* **2004**, *43*, 3762. b) F. Lim, A. M. Sun, *Science* **1980**, *210*, 908.
[9] A. D. Dinsmore, M. F. Hsu, M. G. Nikolaides, M. Marquez, A. R. Bausch, D. A. Weitz, *Science*, **2002**, *298*, 1006.
[10] a) R. Leung, D. Poncelet, R. J. Neufeld, *J. Chem. Technol. Biotechnol.* **1997**, *68*, 37. b) K. Phares, M. Cho, K. Johnson, J. Swarbrick, *Pharm. Res.* **1995**, *12*, 248.
[11] A. Nagayasu, K. Uchiyama, H. Kiwada, *Adv. Drug Delivery Rev.* **1999**, *40*, 75.
[12] T. Nakashima, M. Shimizu, M. Kukizaki, *Adv. Drug Delivery Rev.* **2000**, *45*, 47.
[13] M. D. Louey, M. van Oort, A. J. Hickey, *Pharm. Res.* **2004**, *21*, 1200.
[14] C. Charcosset, I. Limayam, H. Fessi, *J. Chem. Technol. Biotechnol.* **2004**, *79*, 209.
[15] S. Omi, A. Matsuda, K. Imamura, M. Nagai, G.-H. Ma, *Colloid Surf. A* **1999**, *153*, 373.
[16] a) A. M. Ganan-Calvo J. M. Gordillo, *Phys. Rev. Lett.* **2001**, *87*, 274 501. b) I. G. Loscertales, A. Barrero, I. Guerrero, R. Cortijo, M. Marquez, A. M. Ganan-Calvo, *Science* **2002**, *295*, 1695. c) I. Cohen, L. Hui, J. L. Hougland, M. Mrksich, S. R. Nagel, *Science* **2001**, *292*, 265.
[17] S. L. Anna, N. Bontoux, H. A. Stone, *Appl. Phys. Lett.* **2003**, *82*, 364.
[18] J. C. McDonald, D. C. Duffy, J. R. Anderson, D. T. Chiu, H. Wu, O. J. A. Schueller, G. M. Whitesides, *Electrophoresis* **2000**, *21*, 27.
[19] a) A. J. Gijsbertsen-Abrahamse. A. van der Padt, R. M. Boom, *J. Membr. Sci.* **2004**, *230*, 149. b) H. Gau, S. Herminghaus, P. Lenz, R. Lipowsly, *Science* **1999**, *283*, 46.
[20] J. N. Lee, C. Park, G. M. Whitesides, *Anal. Chem.* **2003**, *75*, 6544.
[21] According to the standards of the National Institute of Standards and Technology (NIST) (*Particle Size Characterization*, Special Publication 960-1, January 2001) 'a particle distribution may be considered monodisperse if at least 90 % of the distribution lies within 5 % of the median size.' In order to determine the standard deviations, we fit the experimental histograms of the size of the particles with Gaussian distributions.
[22] a) L. G. M. Gordon, *J. Phys. Chem.* **1981**, *85*, 1753. b) D. Zinemanas, A. Nir, *Int. J. Multiphase Flow* **1995**, *21*, 787.
[23] B. Zheng, J. D. Tice, R. F. Ismagilov, *Adv. Mater.* **2004**, *16*, 1365.
[24] W. Jeong, J. Kim, S. Kim, S. Lee, G. Mensingc, D. J. Beebe, *Lab on a Chip* **2004**, *4*, 576.

Transport Properties in the Rubrene Crystal: Electronic Coupling and Vibrational Reorganization Energy**

By *Demétrio A. da Silva Filho*, *Eung-Gun Kim*, and *Jean-Luc Brédas**

Over the past few years, pentacene has been viewed as the benchmark material for hole mobilities in organic semiconductors, with room-temperature mobilities as high as 35 $cm^2 V^{-1} s^{-1}$ being reported recently.[1] In spite of remarkable progress, a number of issues still remain unclear. For instance, it is still not known what the highest carrier mobility that can be achieved in organic materials is, and what the chemical structures and packing modes that will trigger high mobility are.[2] In this context, the investigation of molecular single crystals can provide a valuable source of information for understanding the microscopic parameters that determine transport efficiency.

Rubrene, a tetraphenyl derivative of tetracene, has lately been gaining much attention.[3–7] Due to the bulky phenyl substituents attached to the side of the tetracene backbone (see Fig. 1), weak intermolecular interactions, and as a result small carrier mobilities, are a priori expected in this system. However, most interestingly, very recent measurements on ultrapure single crystals indicate a field-induced hole mobility of up to 20 $cm^2 V^{-1} s^{-1}$ at room temperature.[7] Therefore, in the present work, we use quantum-chemical calculations of the electronic (band) structure and vibrational reorganization energy of rubrene to elucidate the origin of these large hole mobilities, and of their marked anisotropy along the crystallographic axes;[7] comparison is also made to tetracene and pentacene.

In ultrapure single crystals at low temperature, the electronic coupling between adjacent molecules (that is, the interchain transfer integral, t) is the key parameter in describing the band-like, intrinsic transport properties;[8–10] knowledge of the

[*] Prof. J.-L. Brédas, Dr. D. A. da Silva Filho, Dr. E.-G. Kim
School of Chemistry and Biochemistry
Georgia Institute of Technology
Atlanta, GA 30332-0400 (USA)
E-mail: jean-luc.bredas@chemistry.gatech.edu

[**] This work has been partly supported by the National Science Foundation (through the STC Program under Award DMR-0120967, the MRSEC Program under Award DMR-0212302, and Grant CHE-0342321) and the Office of Naval Research. The authors acknowledge stimulating discussions with V. Coropceanu and J. Cornil.

 © 2005 WILEY-VCH Verlag GmbH & Co. KGaA, Weinheim DOI: 10.1002/adma.200401866